Heliyon 9 (2023) e13502

Contents lists available at ScienceDirect

Heliyon

journal homepage: www.cell.com/heliyon

Research article

Solubility of soil phosphorus in extended waterlogged conditions: An incubation study

Thidarat Rupngam [a,b], Aimé J. Messiga [a,*], Antoine Karam [b]

[a] Agassiz Research and Development Centre, Agriculture and Agri-Food Canada, 6947 Highway 7, P.O. Box 1000, Agassiz, BC V0M 1A0, Canada
[b] Soils and Agri-Food Engineering Department, Laval University, 2425 Rue de l'Université, Québec, QC G1V 0A6, Canada

ARTICLE INFO

Keywords:
Available phosphorus
Dissolved organic carbon
Reduction of ferric (Fe^{3+}) to ferrous (Fe^{2+}) iron
Soil pH
Microbial activity

ABSTRACT

Understanding how extended excess soil moisture exacerbated by extreme weather events affects changes in iron (Fe) chemistry is crucial for assessing environmental risk associated with soil phosphorus (P) in high P soils. The objective of our study was to assess the effects of three soil moisture regimes (field capacity, water saturation, and waterlogging), two Fe^{3+} nitrate level (Fe^{3+} nitrate addition and no Fe^{3+} nitrate addition), and the duration of incubation (0, 3, 7, 14, 21, 28, 35, 49, 63, 90, and 120 days) on the (i) reduction of ferric (Fe^{3+}) to ferrous (Fe^{2+}) iron, (ii) solubility of soil P, and (iii) soil microbial biomass and greenhouse gas emissions. Surface soils (0–20 cm) were collected from a maize silage field located in the Fraser Valley (British Columbia, Canada). Decreased redox potential (Eh) of 155 mV in waterlogged soils coincided with the reduction of Fe^{3+} to Fe^{2+} of about 1190 mg kg^{-1} and an increase in soil pH of 0.8 unit compared to field capacity regime at 120 days after pre-incubation ($P < 0.001$). The increase of pH is due to the microbially-mediated reduction of metal cations which consumes H^+ cations. Water-extractable P (Pw) concentrations increased with increasing soil moisture regimes from 1.47 to 2.27, and 2.58 mg kg^{-1} under field capacity, water saturation, and waterlogged regime respectively. Mehlich-3 extractable P concentrations significantly decreased from 196 to 184 and 172 mg kg^{-1} under water saturation, field capacity, and waterlogged regime respectively. Concomitant to Pw concentrations, microbial biomass carbon and nitrogen as well as DOC, CO_2 and N_2O emissions increased with increasing soil moisture regimes. The Fe^{3+} nitrate addition had an inhibitory effect on Fe reduction, Pw concentration at the first 35 days, and DOC but a stimulating effect on N_2O emission. A high N_2O emission at the first 63 days, CO_2 emission after 35 days, and a non-remarkable concentration of Fe^{2+} at the first 63 days with Fe^{3+} nitrate addition under waterlogged soil suggests that NO_3^- is more preferable than Fe^{3+} as an electron acceptor. Our results showed that soils maintained under extended anoxic conditions could increase the soluble and available P and subsequent risk of P transport to surface and drainage waters, whereas Fe^{3+} nitrate addition could minimize or delay this effect.

1. Introduction

The Fraser valley in British Columbia (BC), Canada, is characterized by unique climatic features in the entire country. Summers are dry, causing farmers to use irrigation water during the growing season which leads to hotspot of nutrients leaching down the soil

* Corresponding author.
E-mail address: aime.messiga@agr.gc.ca (A.J. Messiga).

https://doi.org/10.1016/j.heliyon.2023.e13502
Received 11 January 2023; Received in revised form 27 January 2023; Accepted 1 February 2023
Available online 7 February 2023

profile particularly in horticultural production systems [1]. The Fraser valley is also the seat of the Abbotsford–Sumas Aquifer flowing from British Columbia to Washington creating transboundary issues related to water and groundwater pollution [2]. In addition, 75% of the 1600 mm total precipitations occurs between October and April, leading to leaching of residual soil nitrates and runoff of residual soil phosphates with snowmelt [3]. A major consequence of the heavy rainfall in the region is the excess moisture content of agricultural lands translated as soil water saturation and waterlogging. Many agricultural lands from other parts of the world are prone to flooding during rainy season and spring snowmelt. Studies related to P solubility and redox reaction have been conducted for decades. The alteration in soil moisture contents is expected to affect soil phosphorus (P) and iron (Fe) dynamics and the mobility of P within the soil profile as well as soil aggregate stability [4]. Numerous studies reported that atmospheric weather and climate extremes (e.g., droughts, floods) could affect water storage capacity and soil moisture regimes [5] and thus redox conditions. Anoxic soils often result in reductive dissolution of oxyhydroxides and other minerals [6] and P release into soil solutions [7] via the microbially-mediated reduction of Fe^{3+} oxides, the dissolution of Fe phosphate due to increasing pH and the mineralization of soil organic matter.

Phosphorus is an essential element for plant growth, but poses environmental risks when it is present in the soil above critical levels. Studies conducted in the Fraser valley showed that 89% of fields have soil P concentrations in the excess or very high class, between 100 and 350 mg kg^{-1} Mehlich-3 P (P_{M3}) [8]. A study [9] attributed these high P_{M3} values to higher livestock densities and horticultural productions. High water extractable P (Pw) were also measured in maize silage and blueberry fields with concentrations above critical levels of 3.7 mg kg^{-1} [1,10]. A study on calcareous soils conducted in Manitoba reported that the initial soil P concentration is the main cause of P release to floodwater [11].

Excess moisture content results into anoxic soils with reduced or limited dissolved oxygen. These reducing conditions affect the chemistry of metal cations such as Fe which impact the fixation of P, thus increasing P availability and solubility, and the risk of P transport [11,12]. A study [7] reported that P release from acidic and anaerobic soils is closely associated with reductive dissolution of Fe and Mn phosphates. Changes in Fe chemistry and dynamics under anoxic conditions also affect the activity of microorganisms [13]. Microbial reduction of Fe^{3+} to Fe^{2+} coupled to organic carbon, is a dominant process in anoxic soils [14]. The reduction of Fe^{3+} catalyzes the transformation of organic compounds into carbon dioxide (CO_2) emissions [15]. A study [16] reported that the optimum nitrous oxide (N_2O) emissions usually occur under wetter conditions with moisture content >80% water field pore space.

Excess moisture content can also alter water-stable aggregates through their physical disruption [4], which affects the P and Fe forms and thus their solubility. Indeed, P previously fixed and non-available within aggregates could be dissolved and released to the soil solution following the breakdown of macro-aggregates and loss of labile organic soil carbon. Silt and clay particles with P adsorbed on them present within micro- and macro-aggregates could be released following the physical disruption of water-stable aggregates, thus increasing particulate P losses to floodwater. A study [17] found that Pw increased with soil aggregate size and organic matter accumulation under no-till practice.

A study [18] mentioned that NO_3^- is a preferable electron acceptor after O_2 depletion rather than Fe^{3+}. This statement suggests that the presence of NO_3^- and other non-bound P electron acceptors could decrease or delay P release from soil particles into water sources. Indeed, the microorganisms could use these electron acceptors rather than that bound to P such as Fe and Mn. Assessing the effect of excess moisture on P dynamics in acidic and high P soils is crucial. Besides, microbial biomass and greenhouse gas emissions could provide the insight on P immobilization and reduction processes. The objective of our study was to assess the effects of three soil moisture regimes, two Fe^{3+} nitrate level, and the duration of incubation on the (i) reduction of Fe^{3+} to Fe^{2+} iron, (ii) solubility of soil P, and (iii) soil microbial biomass and greenhouse gas emissions. We hypothesized that redox reactions affecting Fe^{3+} in saturated or waterlogged soils (a) increase soluble P and (b) enhance soil microbial biomass and greenhouse gas emissions with increasing the duration of incubation and without Fe^{3+} nitrate addition.

2. Materials and methods

2.1. Site description and soil collection

The experimental site selected for this study is located at Agassiz Research and Development Center, Agriculture and Agri-Food Canada, BC, Canada (49° 14′ 45.4″N; 121° 45′ 37.8″W). The experiment is constituted of three cropping systems including (1) maize silage (*Zea mays* L.) followed by relay winter cover cropping after harvest, (2) continuous grass, and (3) maize silage interseeded with winter cover cropping at six-leaf stage. Three starter P fertilizer rates are applied to the maize silage plots at maize silage seeding including 0 (control), 10, and 20 kg P ha^{-1}. The experiment was designed to assess how balanced P budget contributes to the drawdown of soil P in high legacy P soils. Some slight rusty gray spots in soil from this experiment were observed during spring in 2020, indicating temporary waterlogged soil. Besides, flood hotspot was occurred in this field during autumn 2021, suggesting that the soil could be exposed to excess water in the past and future. The soil belongs to the Monroe series and classified as Typic Dystroxerepts according to U.S. Soil Taxonomy [19] or Gleyed Dystric Brunisol according to Ref. [20]. The local climate is characterized as moderate oceanic with relatively cool and dry summers, and warm and rainy winters (British Columbia). Annual rainfall ranges from 1483 to 1689 mm with the peak of about 280–350 mm received in November. Average daily temperatures range between 3.4 °C in January to 18.8 °C in August (30 years average, 1981–2010, Agassiz CDA station, British Columbia-Canadian Station) [21].

Soils (0–20 cm) were collected in a maize silage interseeded with winter cover cropping at six-leaf stage plot with an application of 10 kg starter P ha^{-1} (more details on soil collection are described in section 2.2.). Soil was sieved (<2 mm) and the initial soil was air-dried in order to determine the main chemical properties of the composite soil as described below (section 2.4.2.): pH, 5.2; total C, 27.6 mg kg^{-1}; total N, 2.9 mg kg^{-1}; total P, 1281 mg kg^{-1}; Pw, 2.3 mg kg^{-1}; P_{M3}, 165 mg kg^{-1}; Al_{M3}, 2041 mg kg^{-1}; Fe_{M3}, 170 mg kg^{-1};

PSI, 8.6%; DPS, 19.6% (Table 1).

2.2. Incubation experiment

A 120-day incubation experiment using three soil moisture regimes (field capacity with normal oxygenation, water saturation in the absence of oxygen, and waterlogging in the absence of oxygen) and two Fe^{3+} nitrate levels (with Fe^{3+} nitrate and no Fe^{3+} nitrate addition) was conducted in three growth chambers (Conviron Adaptis A1000, Winnipeg, Canada). Eleven destructive sampling dates were retained, and the treatments × sampling dates were arranged in a randomized complete block design with three replicates for a total of 198 experimental units (six treatments × eleven sampling dates × three replicates). All Mason jars (198 jars) were pre-incubated in the growth chambers for 7 d. The sampling dates are: 0, 3, 7, 14, 21, 28, 35, 49, 63, 90, and 120 days after pre-incubation (DAI). Approximately 40 kg of sieved (<2 mm) soils were weighed, separated into sets of 20 kg each (for treatments with and no Fe^{3+} nitrate addition). For treatments with Fe^{3+} nitrate addition, 14.47 g [$Fe(NO_3)_3.9H_2O$] was mixed with 20 kg of soil. 170 g of soil was weight and placed in 500 mL Mason jars. The jars were then separated into three groups representing the three moisture regimes: field capacity (60% water-filled pore space), water saturation (100% water-filled pore space), and waterlogging (100% water-filled pore space and a water layer maintained at a level of 2 cm above the soil surface). A bottle top dispenser was used to add distilled water into the Mason Jars, and then the moist soil was mixed with a spatula. The jars containing soils at water saturation and waterlogging were closed with a lid equipped with a rubber septum consisting of two valves for optimizing the anoxic condition. Nitrogen gas was purged into the Mason jars for 2 min at a flow of 15 mL s^{-1} to displace oxygen (O_2). For soils at field capacity, the jars were covered with a parafilm. A needle was used to puncture 9 holes on the parafilm sheet to allow gas exchange. The 198 Mason jars were then arranged in the three growth chambers (in the dark at 22 °C and 70% humidity) with each growth chamber representing one replicate.

2.3. Gas sampling and analyses

At the end of the pre-incubation period of 7 d, gas samples were collected throughout the duration of the incubation on the same set of sampling jars corresponding to 0, 3, 7, 14, 21, 28, 35, 49, 63, 90 and 120 days after incubation. Two sets of gas samples were collected at two times for each defined sampling period: the day before and after 24 h [22]. Briefly, during the preparation phase, the punctured parafilm on Mason jars containing soils at field capacity and the lids on Mason jars containing soils at water saturation and waterlogging were removed, and air inside the jar was mixed using a handheld fan. The sampled jars were tightly closed with a lid equipped with a rubber septum. The headspace of the closed sampled jar was sampled using a 20 mL syringe equipped with BD PrecisionGlide™ Needle, and the gas was injected into a 12 mL pre-evacuated Exetainer vial (Labco, High Wycombe, UK). After 24 h, the headspace of the closed sampled jar was sampled again as described above, and the collected gas was injected into a second pre-evacuated Exetainer vial. At the end of the sampling phase, the lid equipped with the rubber septum was removed, and the air inside the sampling jar was mixed with a handheld fan, and the jar was closed with a punctured parafilm or lid with rubber septum according to the soil moisture regimes as described in section 2.2. (The jars closed by the lid with rubber septum were again purged with nitrogen) until the next sampling date. The concentrations of CO_2 and N_2O in the gas samples were analyzed using a gas chromatograph (Model 3800, Varian Inc., Walnut Creek, CA, USA) equipped with an electron capture detector (N_2O) and a flame ionization detector (CO_2). The calculation of gas emissions was performed by the modified fluxes equation of N_2O–N [23] as described in equation (1) and cumulative gas emissions were calculated by linear interpolations between sampling dates.

$$F_g = \frac{\frac{dG}{dt}\ x\ V_g\ x\ \frac{M_{m,g}}{V_m}\ x\ \frac{M_{m,a}}{M_{m,g}}}{kg\ soil} \quad (1)$$

Table 1
General chemical properties of the soil (0–20 cm).

pH	5.2
Total carbon (TC, mg kg^{-1})	27,600
Total nitrogen (TN, mg kg^{-1})	2900
Total phosphorus (TP, mg kg^{-1})	1281.3
Total iron (TFe, mg kg^{-1})	33483.1
Carbon to nitrogen ratio (C/N, %)	9.6
Water extractable phosphorus (Pw, mg kg^{-1})	2.3
Mehlich-3 extractable phosphorus (P_{M3}, mg kg^{-1})	164.6
Mehlich-3 extractable aluminum (Al_{M3}, mg kg^{-1})	2041
Mehlich-3 extractable iron (Fe_{M3}, mg kg^{-1})	170
Mehlich-3 extractable calcium (Ca_{M3}, mg kg^{-1})	859
Mehlich-3 extractable magnesium (Mg_{M3}, mg kg^{-1})	131
Phosphorus saturation index (PSI, %)	8.6
Oxalate ammonium phosphorus (P_{Ox}, mg kg^{-1})	1751.2
Oxalate ammonium (Al_{Ox}, mg kg^{-1})	9501.9
Oxalate ammonium (Fe_{Ox}, mg kg^{-1})	12511.5
Degree of phosphorus saturation (DPS, %)	19.6

where G (mol mol^{-1}) is the rate of change of chamber gas concentration, t (hrs) is the sampling time, V_g (L) is the volume occupied by gas, $M_{m,g}$ (g mol^{-1}) is the molecular mass of gas, V_m (m^3 mol^{-1}) is the molecular volume at chamber temperature and barometric pressure, and $M_{m,a}$ (g mol^{-1}) is the molecular mass of the atom (N_2O–N, CO_2–C and CH_4–C).

2.4. Soil and floodwater sampling

At each of the 11 sampling dates, the corresponding Mason jars were removed from the growth chambers. Water in Mason jar for soils with waterlogged regime was collected using a syringe and stored at −20 °C until subsequent analyses. Soil samples were separated into two parts, one was air-dried and the second was kept frozen until subsequent analyses.

2.4.1. Floodwater analysis

Floodwater samples collected from waterlogged moisture regime treatments were thawed at room temperature. They were analyzed for P concentration using the colorimetric blue method [31], for DOC as described below (section 2.4.2.), and for Fe, Mn, Zn, Cu, S, Na, Mg, Ca, K, and Sr by inductively coupled plasma optical emission spectrometry.

2.4.2. Physico-chemical analysis

On air-dried soils, pH and EC were measured in deionized water with a 1:2 soil/solution ratio using a pH meter [24]. The total C and N content in the soils were determined using a CNS analyzer (LECO's TruMac CNS macro analyser). The dissolved organic carbon (DOC) was determined by high-temperature catalytic oxidation method using a Shimadzu TOC-L CPN Analyzer with Total Nitrogen Unit TNM-L & ASI-L Autosampler. Briefly, 2.5 g of air-dried soil was shaken with 25 mL of deionized water in 50 mL centrifuged tubes for 15 min on a reciprocating shaker at a speed of 200 rev min^{-1}, centrifuged at 4200 rpm for 10 min, and filtered through 0.45 μm. The supernatants were stored in the dark at −20 °C prior to analysis [25]. The water-extractable P (Pw) was measured using the method of [26]. The Mehlich-3 extractable P (P_{M3}), Fe (Fe_{M3}), and aluminum (Al_{M3}) were measured as described by Ref. [27]. The acid ammonium oxalate extractable P (P_{OX}), aluminum (Al_{OX}), and iron (Fe_{OX}) was determined as described by Ref. [28]. The total P (TP) and total iron (TFe) were determined by the lithium metaborate fusion method using a Claisse M4 model fluxer (Claisse, Quebec) as described by Ref. [29]. Total organic P (TOP) was determined by the ignition method as described by Ref. [30]. The concentration of Pw and TOP was measured by the colorimetric blue method [31]. Total inorganic P (TIP) was calculated by subtracting TOP from TP. The concentrations of P_{M3}, Fe_{M3}, Al_{M3}, TP, P_{OX}, Al_{OX}, and Fe_{OX} were measured using an inductively coupled plasma optical emission spectrometer (ICAP 7000 series, Thermo Scientific). The degree of P saturation (DPS) [32] and P saturation index (PSI) [33] were obtained by equations (2) and (3) respectively:

$$DPS = \frac{P_{ox}}{\alpha_m(Al_{ox} + Fe_{ox})}\ x\ 100 \tag{2}$$

$$PSI = \frac{P_{M3}}{Al_{M3}}\ x\ 100 \tag{3}$$

where P_{ox}, Al_{ox}, and Fe_{ox} are oxalate extractable P, Al, and Fe (mmol kg^{-1}). α_m is the maximum sorption coefficient and an average α_m value of 0.5 was used [34].

The analysis of Fe^{2+} and Fe^{3+} in the soil samples collected at 0, 63, 90, and 120 d was carried out according to Ref. [35]. Briefly, frozen soils were thawed at room temperature for about 30 min, then 0.5 g of thawed soil was mixed with 7.5 mL of 0.5 M HCl in centrifuge tubes to prevent oxidation of Fe^{2+}. The suspension was shaken on a reciprocating shaker for 1 h, centrifuged at 4200 rpm for 10 min, and the extract was collected and stored at 4 °C for subsequent analysis. The concentration of Fe^{3+} was measured by mixing 100 μL of the extract with 100 μL of 10% hydroxylamine hydrochloride to reduce Fe^{3+} to Fe^{2+}, and 2 mL of a color reagent. The concentration of Fe^{2+} in the extracts was measured at an absorbance of 562 nm using the ferrozine method described by Ref. [36]. As we have got the redox electrodes lately for this experiment, we calculated the redox potential at 0, 63, 90, and 120 d using an equation (4) expressing the relation that exist between Eh, pH and the concentration in Fe^{2+} [37]:

$$E_h = 1.033 - 0.061 \log Fe^{2+} - 0.18\ pH \tag{4}$$

Where E_h is the oxidation-reduction potential (mV), Fe^{2+} is the concentration of ferrous iron (mmol L^{-1}), and pH is the acidity of the soil. The relationship between the calculated E_h and measured E_h using 4 M KCl as reference solution (only from the last samples, n = 18) was performed, see equation (5) with $R^2 = 0.719$:

$$\text{Calculated } E_h = (0.3947 \text{ x Measured } E_h) + 0.0943 \tag{5}$$

This indicates an acceptable positive relationship between the calculated and measured E_h. However, an underestimation of calculated Eh using equation (4) must be considered.

2.4.3. Microbial biomass analysis

Microbial biomass (MB-) C, N, and P were measured on soil samples collected at 0, 63, 90, and 120 d using the chloroform fumigation–extraction method [38]. For MBC and MBN, three sets of 5.0 g moist soils were used for the analysis. The first set was oven-dried at 105 °C for 48 h for moisture content determination. The second set (non-fumigated) was shaken with 25 mL of 0.5 M

K_2SO_4 in 50 mL centrifuge tube at 150 rev min^{-1} for 1 h and filtered through filter paper (Q5 Fisherbrand™ 097902D). The third set (fumigated) was placed into 50 mL glass beakers which were arranged in a desiccator and fumigated with 50 mL ethanol-free chloroform for 24 h in the dark. Fumigated soils were extracted the same way as non-fumigated soils. All extracts were stored at −20 °C until analysis using a TOC analyser (Shimadzu TOC-L CPN Analyzer with Total Nitrogen Unit TNM-L & ASI-L Autosampler). The calculation of MBC and MBN concentrations were performed using extraction coefficients of 0.35 and 0.50 for MBC (K_{EC}) and MBN (K_{EN}), respectively as described by Ref. [38].

For MBP, four sets of 5.0 g moist soils were used for the analysis. The first set was used for determination of moisture content. The second set (fumigated) was processed as described for MBC and MBN. The third and fourth sets (non-fumigation) were placed in 50 mL glass beakers and arranged in a desiccator containing water and soda-lime for 24 h. The third set was transferred in a 50 mL centrifuge tube with 20 mL 0.5 M $NaHCO_3$ buffered at pH 8.5 and 100 μL deionized water. The fourth set was transferred in a 50 mL centrifuge tube with 20 mL 0.5 M $NaHCO_3$ buffered at pH 8.5 and 100 μL of a 250 μg P_i mL^{-1} spiking solution. The mixtures (third and fourth sets) were shaken at 150 rev min^{-1} for 30 min, centrifuged at 3400 rpm for 8 min and filtered through filter paper (Q5 Fisherbrand™ 097902D). The concentration of P in all extracts was determined by the colorimetric blue method [31]. The calculation of MBP concentrations was performed using extraction coefficient of 0.4 (K_{EP}) as described by Ref. [38].

2.5. Statistical analyses

The data was pre-tested with Shapiro-Wilk normality test to determine if it is normally distributed. Natural log function was used to transform non-normal distribution data (if need). All statistical analyses were performed in R software. ANOVA analyses with interactions followed by Tukey's multiple comparison tests (if needed) were used with the significance level of 0.05. The principal components analysis (PCA) was performed using the "FactoMineR" and "factoextra" packages to visualize and identify correlated variables. The function "fviz_pca_biplot" was used to superimpose the biplot of individuals and variables. The correlation test was performed by "corrplot" package. The function "cor.mtest" was used for a significance test, which produces p-values and confidence intervals for each pair of variables.

3. Results

3.1. pH, redox potential, and Fe forms

Soil pH increased with increasing soil moisture regime, but the extent was influenced by the duration of incubation ($P < 0.001$) (Table 2). During the incubation, soil pH was mainly in the order waterlogged > water saturation > field capacity (Fig. 1a). Small variations were observed during the periods 21 and 63 DAI where soil pH decreased across the three moisture regimes then increased except under field capacity. The soil pH decreased with addition of Fe^{3+} nitrate, but the extent varied with the soil moisture regime ($P < 0.001$) and the duration of the incubation ($P < 0.001$) (Table 2). The addition of Fe^{3+} nitrate decreased the soil pH from 4.9 to 4.6 under field capacity and from 5.3 to 5.1 under waterlogged conditions (Fig. 1b and c).

The Eh decreased with increasing soil moisture regime, but the extent varied with the duration of the incubation ($P < 0.001$) (Table 2). During the period 0 to 63 DAI, Eh was in the order field capacity > water saturation = waterlogged, but after that period Eh significantly decreased under waterlogged compared with field capacity (Fig. 1d). During the incubation period, Eh varied from 206 to 270 mV under field capacity, from 212 to 153 mV under water saturation, and from 170 to 48 mV under waterlogged (Fig. 1d). The Eh was high with addition of Fe^{3+} nitrate, but the extent varied with the duration of the incubation ($P < 0.001$) (Table 2). The Eh decreased from 222 to 181 mV with addition of Fe^{3+} nitrate, but increased from 165 to 188 mV without addition of Fe^{3+} nitrate throughout the duration of the incubation (Fig. 1e).

Table 2
Significance (*P*-values) of the effect of moisture content, Fe^{3+} nitrate addition, and sampling dates (time) on soil pH, redox potential, iron forms, available phosphorus, soil microbial biomass, and greenhouse gas emissions.

	Soil pH	Redox potential	Fe^{3+}	Fe^{2+}	Pw	P_{M3}	P in floodwater	CO_2	N_2O	MBC	MBN	MBP
Moisture content (MC)	<0.001	<0.001	<0.001	<0.001	<0.001	<0.001	–	<0.001	<0.001	0.028	0.014	ns
Fe^{3+} nitrate addition (FeN)	<0.001	0.012	ns	ns	<0.001	ns	ns	0.033	<0.001	ns	ns	ns
Time (T)	<0.001	ns	0.006	0.010	<0.001	<0.001	<0.001	<0.001	0.001	ns	0.016	ns
MC × FeN	<0.001	ns	ns	ns	ns	ns	–	ns	<0.001	ns	ns	ns
MC × T	<0.001	<0.001	0.026	<0.001	0.012	<0.001	–	<0.001	<0.001	ns	ns	ns
Fe × T	<0.001	0.049	ns	0.029	<0.001	0.036	ns	0.023	0.023	ns	ns	ns
MC × FeN × T	ns	ns	ns	ns	ns	ns	–	ns	<0.001	ns	ns	ns
N	198	72	72	72	198	198	66	198	198	198	72	72

ns, not significant at $P = 0.05$; Fe^{3+}, ferric iron; Fe^{2+}, ferrous iron; Pw, water extractable phosphorus; P_{M3}, mehlich-3 extractable phosphorus; P in water flooded layer under waterlogged soil; CO_2, N_2O, CH_4, carbon dioxide, nitrous oxide, and methane emission; MBC, MBN, MBP, microbial biomass C, N, and P.

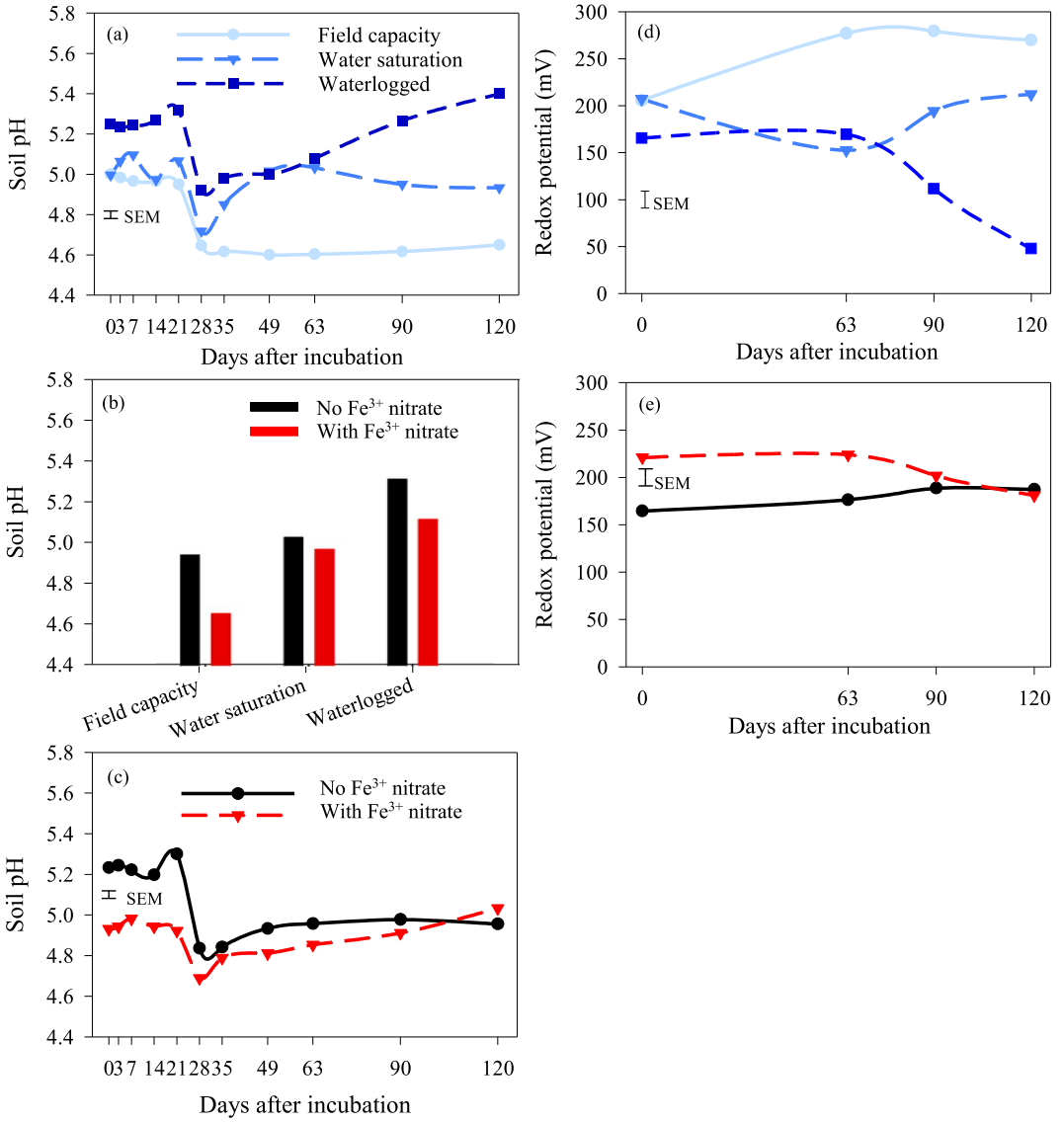

Fig. 1. Soil pH as influenced by (a) moisture regime (field capacity, water saturation, waterlogged), (b) moisture regime and Fe^{3+} nitrate addition, (c) incubation time, and (d, e) the redox potential of the soil during 120 days after pre-incubation in the growth chamber. Error bars represent standard errors of the means [SEM, n1 (represents soil pH values) = 198, df_a = 12, $df_{b,c}$ = 120; n2 (represents redox potential values) = 72, df = 34)].

The concentration of Fe^{3+} decreased with increasing moisture, but the extent varied with the duration of the incubation (P = 0.042) (Table 2). The concentration of Fe^{3+} varied from 1989 at 0 DAI and 1701 mg kg^{-1} at 63 and 90 DAI under field capacity; from 1824 at 0 DAI to 1411 mg kg^{-1} at 90 DAI under water saturation; and from 1661 at 0 DAI to 528 mg kg^{-1} at 120 DAI under waterlogged (Fig. 2a). The concentration of Fe^{2+} increased with increasing moisture, but the extent varied with the duration of the incubation (P < 0.001) (Table 2). The concentration of Fe^{2+} varied from 45 mg kg^{-1} at 0 DAI across all moisture regimes and 1291 mg kg^{-1} at 120 DAI under waterlogged, 664 mg kg^{-1} at 63 DAI and 78 mg kg^{-1} at 120 DAI under water saturation, but remained constant around 46 mg kg^{-1} throughout the incubation period under field capacity (Fig. 2b). The concentration of Fe^{2+} increased during the incubation, but the extent was influenced by the addition of Fe^{3+} nitrate (P = 0.029). The concentration of Fe^{2+} was 46 mg kg^{-1} at 0 DAI and 473 mg kg^{-1} at 120 DAI over the two Fe^{3+} nitrate levels (Fig. 2c). In contrast, there was a difference in the concentration of Fe^{2+} between the two Fe^{3+} nitrate levels with 613 mg kg^{-1} without addition of Fe^{3+} nitrate and 82 mg kg^{-1} with addition of Fe^{3+} nitrate at 63 DAI and 388 mg kg^{-1} without addition of Fe^{3+} nitrate and 260 mg kg^{-1} with addition of Fe^{3+} nitrate at 90 DAI of incubation (Fig. 2c).

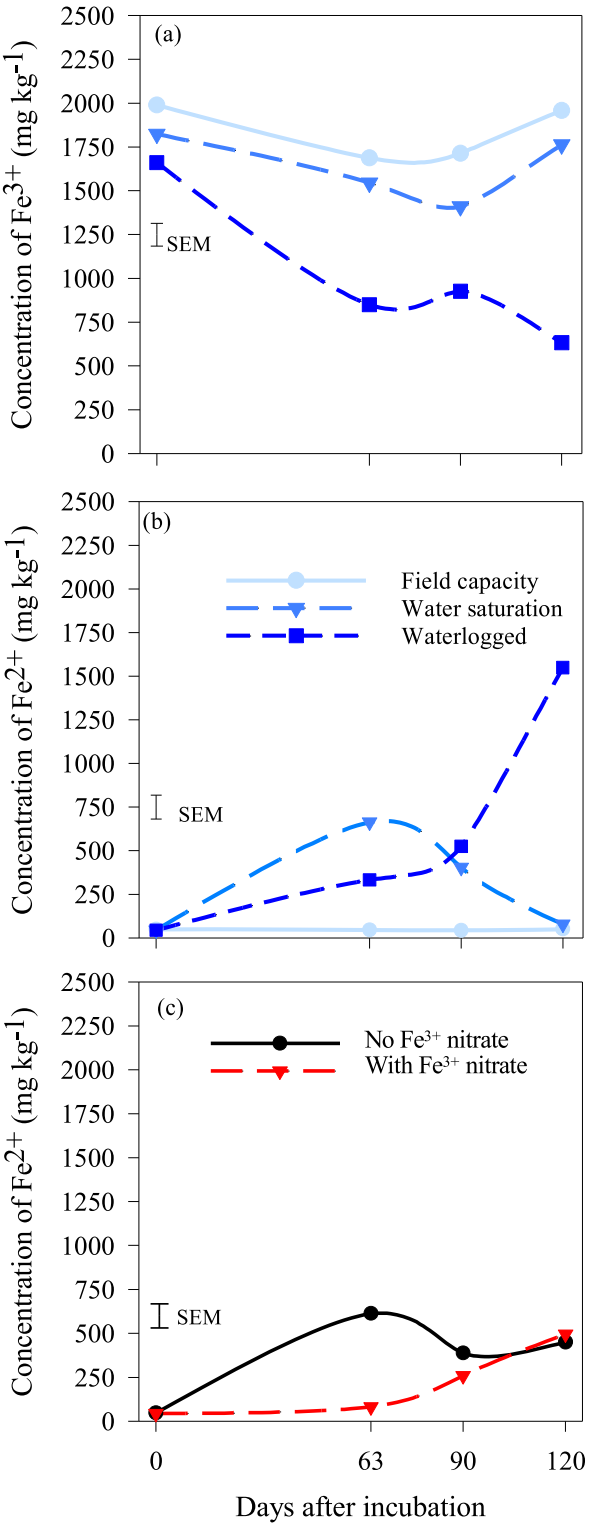

Fig. 2. Effects of soil moisture regime (field capacity, water saturation, waterlogged) on the concentrations of (a) ferric iron (Fe^{3+}) and (b) ferrous iron (Fe^{2+}). Effects of Fe^{3+} nitrate addition on the concentration of ferrous iron (Fe^{2+}) during 120 days after pre-incubation in the growth chamber (c). Error bars represent standard errors of the means (SEM, n = 72, df = 36).

3.2. Water extractable P and Mehlich-3 extractable P

The concentration of Pw increased with soil moisture regime, but the extent was influenced by the duration of the incubation ($P = 0.012$) (Table 2). The Pw varied from 0.99 mg kg^{-1} to 1.79 mg kg^{-1} under field capacity, from 1.17 mg kg^{-1} to 3.12 mg kg^{-1} under water saturation and from 1.88 mg kg^{-1} to 3.08 mg kg^{-1} under waterlogged (Fig. 3a). Three patterns were observed with the trend of Pw among the three moisture regimes with time: the first pattern occurred between 0 and 21 DAI during which Pw was similar across soils under field capacity and water saturation but lower than waterlogged; the second pattern occurred between 21 DAI and 35 DAI where there was an increase in Pw across soils under water saturation and waterlogged while Pw remained constant in soils under field capacity; the third pattern occurred between 35 DAI and 120 DAI where Pw was similar across water saturation and waterlogged moisture regimes but greater than field capacity (Fig. 3a). The concentration of Pw decreased with addition of Fe^{3+} nitrate, but the extent varied with the duration of incubation ($P < 0.001$) (Table 2). The concentration of Pw increased from 1.0 mg kg^{-1} at 0 DAI to 2.8 mg kg^{-1} at 63 DAI, then decreased to 1.7 mg kg^{-1} at 120 DAI with addition of Fe^{3+} nitrate (Fig. 3b). The concentration of Pw decreased from 3.1 mg kg^{-1} at 0 DAI to 1.8 mg kg^{-1} at 120 DAI without addition of Fe^{3+} nitrate (Fig. 3b).

The concentration of P_{M3} decreased with increasing soil moisture regime, but the extent was influenced by the duration of the incubation ($P < 0.001$) (Table 2). During the period 0 and 63 DAI of incubation, the concentration of P_{M3} decreased from 187 to 160 mg kg^{-1} over the three moisture regimes (Fig. 3c). In contrast, during the period 63 and 90 DAI of incubation the concentration of P_{M3} increased from 160 to 233 mg kg^{-1} in soils under field capacity and water saturation, but to 176 mg kg^{-1} only in soils under waterlogged moisture regime (Fig. 3c). During the period 90 to 120 DAI, the concentration of P_{M3} remained constant in soils under field capacity and water saturation, but decreased to 148 mg kg^{-1} in soils under waterlogged moisture regime (Fig. 3c). The concentration of P_{M3} varied with addition of Fe^{3+} nitrate, but the extent was influenced with the duration of incubation ($P = 0.036$) (Table 2). During the period 0 and 35 DAI, the concentration of P_{M3} decreased from 188 to 171 mg kg^{-1} in soils with and without Fe^{3+} nitrate addition. The concentration of P_{M3} was significantly greater in soils with addition of Fe^{3+} nitrate compare with soils without addition of Fe^{3+} nitrate at 49, 63 and 90 DAI (Fig. 3d). We also observed a trend of increasing P_{M3} between 63 and 90 DAI in soils with addition of Fe^{3+} nitrate and those without addition of Fe^{3+} nitrate.

We observed an increase in P in floodwater under waterlogged soil from 0.2 mg L^{-1} at 0 DAI to 0.7 mg L^{-1} at 120 DAI (Fig. 4).

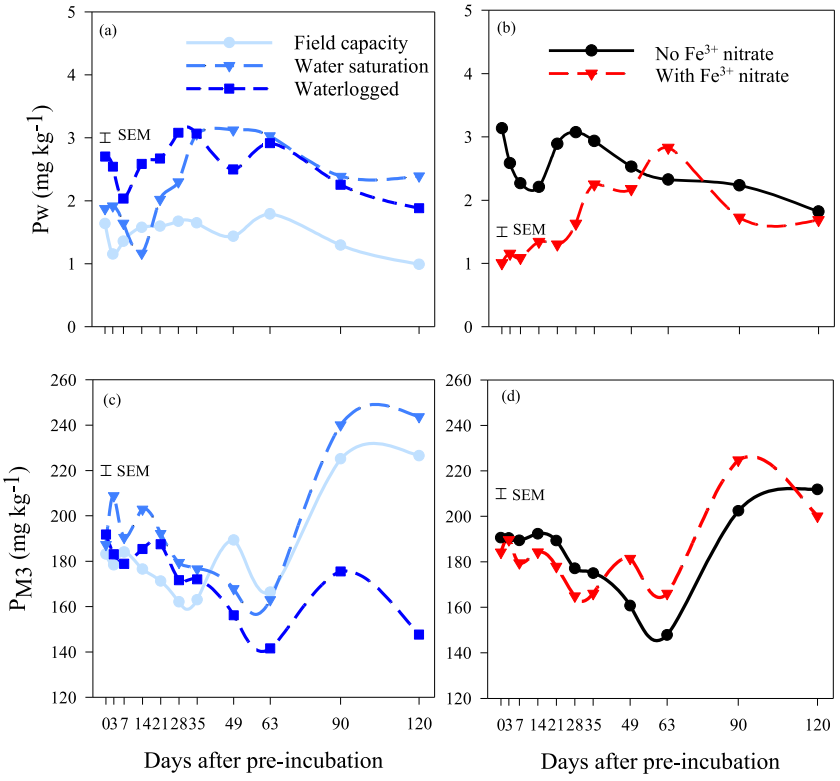

Fig. 3. Effects of soil moisture regimes (field capacity, water saturation, waterlogged) and Fe^{3+} nitrate addition on the concentrations of (a, b) water extractable phosphorus (P_w) and (c, d) Mehlich-3 extractable phosphorus (P_{M3}) during 120 days after pre-incubation period in the growth chamber. Error bars represent standard errors of the means (SEM, n = 198 and df = 120).

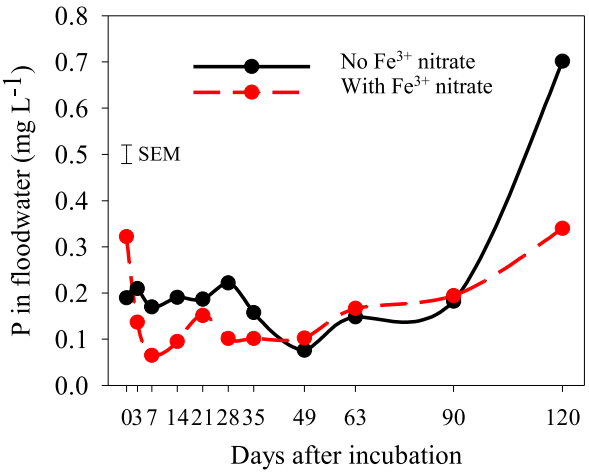

Fig. 4. Effects of Fe^{3+} nitrate addition (no Fe nitrate and with Fe nitrate) on P concentration in floodwater measured by colorimetric blue method during 120 days after pre-incubation. Error bars represent standard errors of the means (SEM, n = 66, df = 44).

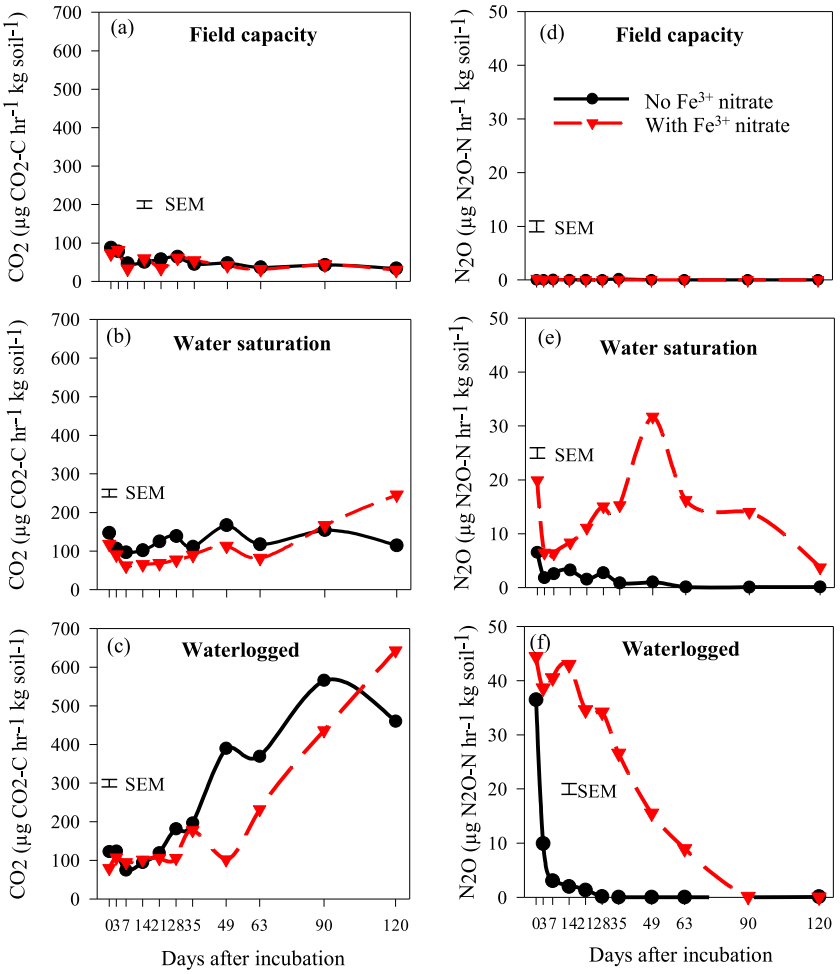

Fig. 5. Effect of soil moisture regimes (field capacity, water saturation, waterlogged) and Fe^{3+} nitrate additions (no Fe^{3+} nitrate and with Fe^{3+} nitrate) on (a, b, c) CO_2 and (d, e, f) N_2O emissions during 120 days after pre-incubation period in the growth chamber. Error bars represent standard errors of the means (SEM, n = 198, df = 120).

3.3. Evolution of CO_2–C and N_2O–N during the incubation period

The CO_2 emission varied with soil moisture regime, but the extent was influenced by the duration of incubation ($P < 0.001$) (Table 2). The CO_2 emissions decreased from 78 μg CO_2–C hr^{-1} $kg\ soil^{-1}$ at 0 DAI to 32 μg CO_2–C hr^{-1} $kg\ soil^{-1}$ at 120 DAI under field capacity (Fig. 5a); increased from 132 μg CO_2–C hr^{-1} $kg\ soil^{-1}$ at 0 DAI to 180 μg CO_2–C hr^{-1} $kg\ soil^{-1}$ at 120 DAI under water saturation (Fig. 5b); increased from 100 μg CO_2–C hr^{-1} $kg\ soil^{-1}$ at 0 DAI to 552 μg CO_2–C hr^{-1} $kg\ soil^{-1}$ at 120 DAI under waterlogged moisture regime (Fig. 5c). Furthermore, the CO_2 emission decreased with addition of Fe^{3+} nitrate, but the extent was influenced by the duration of incubation ($P = 0.023$) (Table 2). The CO_2 emission was on average 108 μg CO_2–C hr^{-1} $kg\ soil^{-1}$ for the two Fe^{3+} nitrate levels from 0 to 35 DAI of incubation, but 86–307 μg CO_2–C hr^{-1} $kg\ soil^{-1}$ without Fe^{3+} nitrate addition and 201–254 μg CO_2–C hr^{-1} $kg\ soil^{-1}$ with addition of Fe^{3+} nitrate between 49 and 120 DAI (Fig. 5a,b,c).

The N_2O emission increased with addition of Fe^{3+} nitrate, but the extent was influenced by the moisture regime and duration of incubation (Fe × MC × T, $P < 0.001$) (Table 2). Overall, N_2O emissions remained constant and close to 0 μg N_2O–N hr^{-1} $kg\ soil^{-1}$ during the incubation period in soils under field capacity (Fig. 5d); decreased from 7 to 0.1 μg N_2O–N hr^{-1} $kg\ soil^{-1}$ during the incubation without Fe^{3+} nitrate addition, and varied from 4 to 32 μg N_2O–N hr^{-1} $kg\ soil^{-1}$ with Fe^{3+} nitrate addition under water saturation, (Fig. 5e). In contrast, N_2O emissions decreased from 36 μg N_2O–N hr^{-1} $kg\ soil^{-1}$ at 0 DAI to 9 μg N_2O–N hr^{-1} $kg\ soil^{-1}$ at 3 DAI and remained constant during the rest of the incubation without Fe^{3+} nitrate addition, and 44 μg N_2O–N hr^{-1} $kg\ soil^{-1}$ at 0 DAI to 8 μg N_2O–N hr^{-1} $kg\ soil^{-1}$ at 90 DAI with addition of Fe^{3+} nitrate under waterlogged moisture content (Fig. 5f).

3.4. Evolution of MBC, MBN, and MBP during the incubation period

The MBC increased with increasing soil moisture regime ($P < 0.05$) (Table 2). The MBC varied from 175 μg g^{-1} soil at 0 DAI to 111 μg g^{-1} soil at 120 DAI in soils under field capacity; from 173 at 0 DAI to 150 at 120 DAI in soils under water saturation; from 258 μg g^{-1} soil at 0 DAI to 183 μg g^{-1} soil at 120 DAI in soils under waterlogged moisture regime (Fig. 6a).

The MBN increased with increasing soil moisture regime ($P < 0.05$), but decreased during incubation period ($P < 0.05$) (Table 2). The MBN varied from 100 μg g^{-1} soil at 0 DAI to 15 μg g^{-1} soil at 120 DAI in soils under field capacity; from 64 μg g^{-1} soil at 0 DAI to 28 μg g^{-1} soil at 120 DAI with a maximum of 104 μg g^{-1} soil at 63 DAI in soils under water saturation; from 206 μg g^{-1} soil at 0 DAI to 40 μg g^{-1} soil at 120 DAI of incubation in soils under waterlogged moisture regime (Fig. 6b).

The MBP was not significantly affected by the soil moisture regime, Fe^{3+} nitrate addition, and the duration of incubation (Table 2). On average, MBP was 250 μg g^{-1} soil during the incubation experiment.

3.5. Evolution of DOC during the incubation period

The concentration of DOC increased with increasing soil moisture regime, but the extent varied during the incubation period ($P < 0.001$) (Table 3). The DOC decreased from 148 mg kg^{-1} at 0 DAI to 122 mg kg^{-1} at 120 DAI under field capacity; 155 mg kg^{-1} at 0 DAI to 140 mg kg^{-1} at 120 DAI under water saturation; but increased from 159 mg kg^{-1} at 0 DAI to 195 mg kg^{-1} at 120 DAI under waterlogged moisture regime (Fig. 7a). The concentration of DOC decreased with addition of Fe^{3+} nitrate, but the extent varied during the incubation ($P < 0.05$) (Table 3). The DOC in soils with or without Fe^{3+} nitrate addition was 141 and 167 mg kg^{-1} at 0 DAI; 142 and 180 mg kg^{-1} at 63 DAI; 145 and 170 mg kg^{-1} at 90 DAI; but 153 and 151 mg kg^{-1} at 120 DAI, respectively (Fig. 7b).

The concentration of DOC in the floodwater decreased with Fe^{3+} nitrate addition, but the extent varied with increasing duration of incubation (Table 3). The concentration of DOC in the floodwater with or without addition of Fe^{3+} nitrate was 5 and 7 mg kg^{-1} at 0 DAI; 8 and 51 mg kg^{-1} at 63 DAI; 25 and 71 mg kg^{-1} at 90 DAI; and 56 and 98 mg kg^{-1} at 120 DAI, respectively (Fig. 7c).

3.6. Relationship between the parameters

Principal component analysis-Biplot (PCA) showed that the studied variables were distinctively divided in two groups: (i) the variables related to field capacity regime and (ii) the variables related to waterlogged regime (Fig. 8). The Eh, EC, and P_{M3} were related to field capacity moisture regime. The P_w, soil pH, DOC, Fe^{2+}, CO_2, N_2O, and C to N ratio were related to waterlogged moisture regime.

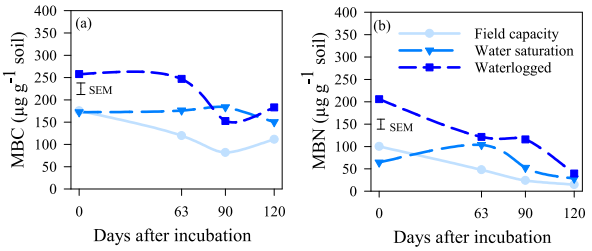

Fig. 6. Effects of soil moisture regime (field capacity, water saturation, waterlogged) on (a) microbial biomass carbon (MBC) and (b) microbial biomass nitrogen (MBN) during 120 days after pre-incubation period in the growth chamber. Error bars represent standard errors of the means (SEM, n = 72, df = 48).

Table 3
Soil properties as affected by moisture content, Fe^{3+} nitrate addition, and sampling dates (time).

	TC	TN	C-to-N	DOC	DPS	Fe_{M3}	Al_{M3}	PSI
Moisture content (MC)								
Field capacity	26.9	2.8	9.7	133.5	20.7	238	1878	9.5
Water saturation	27.8	2.8	10.0	157.1	21.7	310	1919	9.9
Waterlogged	27.5	2.7	10.1	177.7	21.7	299	1927	9.1
SEM (MC)	*0.21*	*0.03*	*0.13*	*2.61*	*0.46*	*7.52*	*20.83*	*0.15*
Fe^{3+} nitrate addition (FeN)								
No Fe^{3+} nitrate	27.9	2.8	9.9	167.1	22.2	294	1884	9.7
With Fe^{3+} nitrate	26.8	2.7	10.0	145.1	20.5	270	1932	9.3
SEM (FeN)	*0.17*	*0.02*	*0.11*	*1.83*	*0.38*	*6.14*	*17.01*	*0.12*
Time (T)								
0	26.9	2.6	10.6	154.0	21.3	254	1864	9.8
3	27.2	2.7	10.4	–	21.4	215	1919	9.4
7	27.5	2.8	9.8	–	20.6	186	2113	8.6
14	27.9	2.9	9.8	–	21.3	190	2116	8.7
21	27.3	2.9	9.6	–	21.9	302	1932	9.8
28	26.9	2.8	9.6	–	22.3	303	1622	10.3
35	28.4	2.9	9.8	–	22.3	310	1609	10.3
49	27.7	2.9	9.7	–	22.1	339	1663	9.7
63	27.4	2.8	9.9	160.8	22.2	347	1656	9.4
90	27.9	2.8	10.0	157.5	18.7	324	2224	9.6
120	26.2	2.6	10.1	152.1	21.0	331	2273	8.8
SEM (T)	*0.40*	*0.05*	*0.22*	*0.45*	*0.46*	*10.01*	*39.82*	*0.19*
P values								
MC	0.040	ns	ns	<0.001	ns	<0.001	ns	<0.001
FeN	0.001	0.006	ns	<0.001	ns	0.019	ns	0.002
MC × FeN	0.002	0.001	ns	ns	ns	0.003	ns	ns
T	0.018	<0.001	0.029	ns	<0.001	<0.001	<0.001	<0.001
MC × T	ns	0.046	ns	<0.001	ns	0.001	ns	<0.001
FeN × T	ns	ns	ns	0.019	ns	<0.001	ns	<0.001
MC × FeN × T	ns	ns	ns	ns	ns	0.004	ns	ns
N	198	198	198	72	196	198	198	198

ns, not significant at $P = 0.05$; *SEM,* standard errors of the means; TC, total carbon (mg kg^{-1}); TN, total nitrogen (mg kg^{-1}); C-to-N, carbon to nitrogen ratio (%); DOC, dissolved organic carbon (mg kg^{-1}); DPS, degree of phosphorus saturation (%); Fe_{M3} and Al_{M3}, Mehlich-3 extractable iron and aluminium (mg kg^{-1}); PSI, phosphorus saturation index (%).

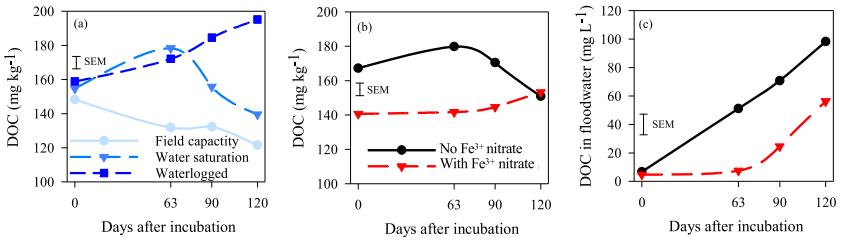

Fig. 7. Dissolve organic carbon (DOC) in soils (a,b) and (c) in floodwater as affected by soil moisture regime (field capacity, water saturation, waterlogged) and Fe^{3+} nitrate additions (no Fe^{3+} nitrate and with Fe^{3+} nitrate) during 120 days after pre-incubation period in the growth chamber. Error bars represent standard errors of the means (SEM, n1 (represents soil moisture effects) = 72, df = 48; n2 (represents iron addition effects) = 24, df = 16).

The duration of incubation affected the elements present in the floodwater ($P < 0.001$). We found the presence of Zn, K, Sr, Ca, and Cu at 0 and 63 DAI, Mg, Na, S, Mn, and inorganic phosphorus at 60 and 90 DAI, and Fe, DOC, and total P at 120 DAI (Fig. 9).

4. Discussion

4.1. Reduction of Fe and effects on soil pH and Eh

The increase of soil pH obtained under waterlogged moisture regime is the result of reducing conditions leading to the change of Fe^{3+} into Fe^{2+} [39]. A study [40] conducted on different paddy soils during submerging/draining alternation found that the reduction of Fe^{3+} into Fe^{2+} plays a leading role in increasing soil pH. The reaction consumes H^+ cations in the soil solution mainly from Fe^{3+} oxide reduction relative to the reduction of Mn^{4+}/Mn^{3+} oxides and SO_4^{2+}/H_2S [13]. In contrast, decreased soil pH under field capacity is due to aerobic conditions leading to production of H^+ [41]. Changes in soil pH and Fe forms with varying moisture regimes were also

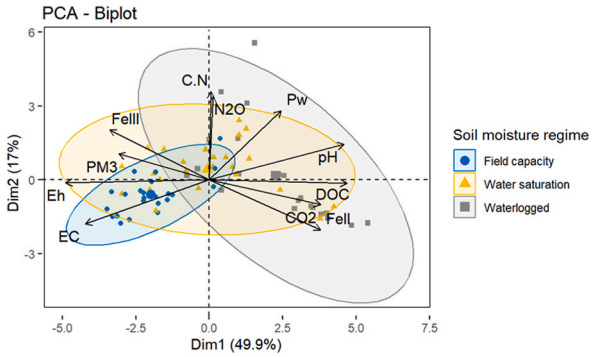

Fig. 8. Principal component analysis (PCA)-Biplot reveals the projection of the variables determined from incubated soil in the growth chamber, grouped according to soil moisture regime (field capacity, water saturation, waterlogged). C.N = carbon-to-nitrogen ratio.

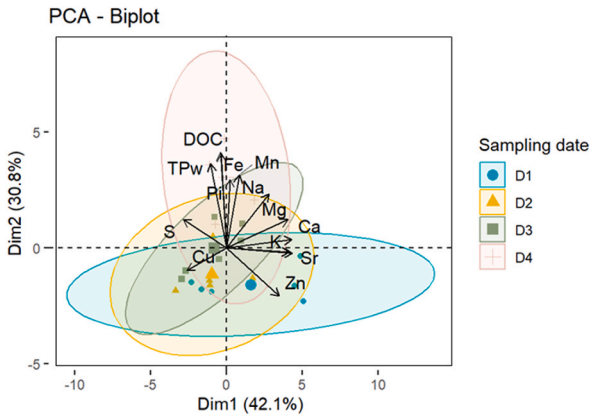

Fig. 9. PCA-Biplot demonstrates the projection of the variables of the elements presented in the floodwater under waterlogged soils and the other five variables (CO_2, MBC, MBN, MBP, and Fe^{2+}). The variables were grouped according to sampling dates (D1 = 0 DAI, D2 = 63 DAI, D3 = 90 DAI and D4 = 120 DAI). TPw = total phosphorus in floodwater and Pi = inorganic phosphorus.

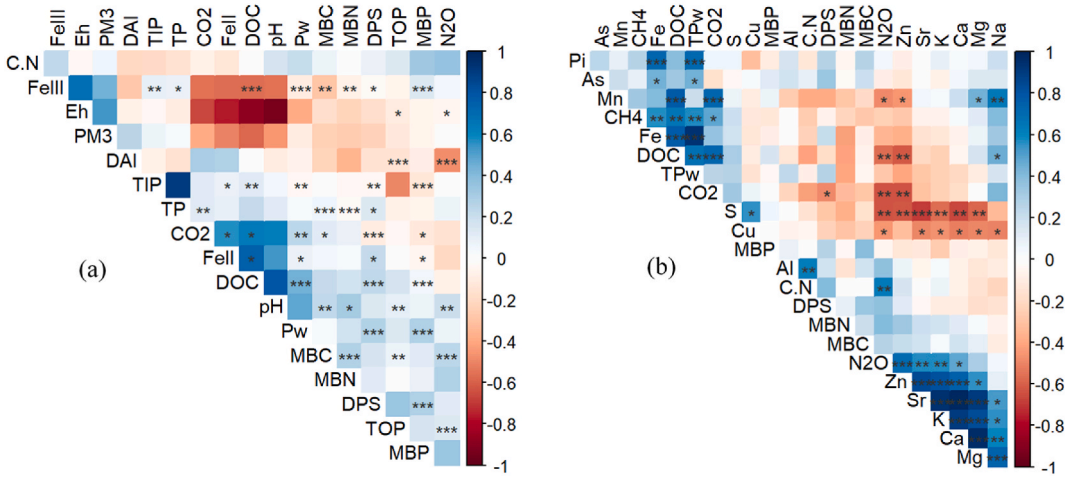

Fig. 10. Correlation between the variables as determined by Pearson's correlation coefficient (Significant codes: 0 '***' 0.001 '**' 0.01 '*' 0.05). The colors and their intensity represent the correlation coefficient: blue indicate the positive correlation and red indicate the negative correlation. (a) variables obtained from soil samples and (b) variables obtained from floodwater and some variables from soil samples. TPw = total phosphorus in floodwater measured by ICAP, C.N = carbon-to-nitrogen ratio, Pi = inorganic phosphorus in floodwater measured by colorimetric blue method, and TIP = total inorganic phosphorus. (For interpretation of the references to color in this figure legend, the reader is referred to the Web version of this article.)

followed by changes in Eh (Fig. 10a) which is due to changes in O_2 concentrations, H^+ concentrations, and electron exchange in the soil. Studies showed that O_2 is rapidly depleted from the soil following flooding because its diffusion times in water are four orders of magnitude lower than those in air [42] while microbial respiration persists. The increased Eh following addition of Fe^{3+} nitrate during the first 63 DAI of the incubation could be due to Fe^{3+} nitrate. Fe^{3+} nitrate inhibited the iron reduction up to 63 DAI. This inhibition decreases the consumption of H^+ and consequently results in lower soil pH, lower Fe^{2+} concentrations and higher Eh, as confirmed by the negative relationship between pH and Eh and between Fe^{2+} and Eh (Fig. 10a). The use of the added nitrate as an electron acceptor could explain this decrease of Fe^{2+} concentration with Fe^{3+} nitrate addition.

4.2. Solubility of P under varying moisture regimes

Increased Pw concentrations under water saturation and waterlogged moisture regimes (Fig. 3a) could be due to the physical disruption of soil aggregates by the excess water [4], which solubilizes the P that was previously protected and not exchangeable. A study conducted in Quebec showed that Pw concentrations increase with increasing water-stable aggregates size classes [17]. The P ions at the solid-to-solution interface are in equilibrium and these ions move from one phase to another through diffusion following a concentration gradient [43]. This equilibrium is affected by many processes including adsorption-desorption and mineralization-immobilization. The excess water around solid particles derived from the physically disturbed aggregates dilutes the P ions and decreases their concentration in the solution. The result is a concentration gradient at the solid-to-solution interface which leads to the desorption of P ions from the solid phase into the solution. Increased Pw concentrations under water saturation and waterlogged moisture regimes could also be due to the dissolution of previously precipitated amorphous solids [13,44]. This assumption is supported by increased soil pH observed under these moisture regimes leading to consumption of H^+ (Fig. 1a and b). Increased soil pH as a result of the consumption of H^+ in anaerobic conditions is a feedback mechanism of the reduction of Fe^{3+} to Fe^{2+} as well as other soil components including Mn^{4+}/Mn^{3+} oxides and SO_4^{2+}/H_2S [6,13], which could release bound P into pore water and floodwater. In addition, results of Pearson's correlation showed a positive and strong correlation between Pw concentrations and soil pH for this soil with pH range from 4.6 to 5.4 (Fig. 10a). The role of excess water on the solubilization of P ions from reduction reaction is further highlighted by the addition of Fe^{3+} nitrate which led to decreased Pw concentrations (Fig. 3b). Previous studies using soils from the Fraser valley have shown that the role of pedogenetic Fe oxides on P sorption and fixation in these soils is minimal [10]. Besides, the added Fe^{3+} nitrate acts as available electron acceptors which could be used by microorganisms after O_2 depletion [18].

We expected increased P_{M3} concentrations under water saturation and waterlogged moisture regimes concomitant with increased Pw concentrations. To our surprise, P_{M3} concentrations were similar in soils under field capacity and water saturation moisture regimes, but lower in soils under waterlogged moisture regime (Fig. 3c). It is possible that increased P_{M3} in soils under field capacity and water saturation moisture regimes in the later period of the incubation was due to more P from the solid phase becoming extractable. The maintenance of these moisture regimes during an extended period enabled reducing conditions that enhanced P desorption and dissolution as well as mineralization of organic and microbial P [43]. In contrast to field capacity and water saturation moisture regimes, it is possible that the decreased P_{M3} under waterlogged moisture regime is due to the removal of P with floodwater. Indeed, floodwater in soils under waterlogged moisture regime was decanted, collected and analyzed separately (Fig. 4). Our data also show high concentrations of other elements including Fe, DOC, Mn, Na, S, Mg, Ca, K, Sr, Zn, and Cu in the floodwater which is in line with the effects of reducing conditions [41] that prevailed during the incubation (Fig. 9).

4.3. Effects of soil moisture regimes and Fe^{3+} nitrate addition on soil microbial activity

Increased CO_2 emissions with increased moisture regimes and time (Fig. 5b and c) is due to soil microbial activity taking place under anaerobic conditions. The trend of CO_2 emissions is in line with increased MBC and MBN under water saturation and waterlogged moisture regimes (Fig. 6a and b) as well as DOC (Fig. 7a). The release of C from waterlogged soil could also stimulate CO_2 emission [45]. The CO_2 emissions under water saturation and waterlogged moisture regimes could be the result of anaerobic conditions leading to the reduction of Fe^{3+} as well as Mn^{4+} which is also supported by increased soil pH, Pw concentration, and DOC (Fig. 10a and b). It is well known that the reduction of metal cations by microorganisms catalyzes the transformation of organic compounds into CO_2 [15].

Increased MBC and MBN under waterlogged regime represent the immobilization of inorganic C and N in microbial biomass. A study in 2022 [46] demonstrated that the MBC and MBN in paddy soils are twice more than that in upland soils. This could be explained by microbial biomass turnover, Fe and Mn oxidation-reduction dynamics which stabilize C, and high microbial substrate use efficiency [46]. The microbial C:N:P stoichiometry affects mineralization of organic C, N, and P in soil [47] by releasing enzymes. This suggest that the enzymatic activities could involve in P release under waterlogged regime.

Increased concentrations of DOC with increased moisture regimes represents an important source of organic C for decomposition, mineralization, and fermentation and therefore substrates for soil microbial activity [48]. Increased DOC under water saturation and waterlogged moisture regimes could be the result of the physical disruption of water-stable aggregates. Increased concentrations of DOC in soils submitted to excess moisture regimes are reported in several studies. We found that the concentration of DOC was positively related to soil pH, Pw, and Fe^{2+}, but negatively to P_{M3}, Eh, and Fe^{3+} (Fig. 10a). Our results indicate that the reduction of Fe^{3+} to Fe^{2+} can play a role in the increase of the concentrations of DOC and Pw as a feedback mechanism of nutrient-mediated metabolic boost of organic matter degrading microorganisms. The role of the reduction process of Fe^{3+} to Fe^{2+} on the release of DOC under excess moisture regimes is further highlighted by the decreased concentrations of DOC in soils under field capacity due to the adsorption of organic matter compounds onto Fe^{3+} as well as Mn^{4+} oxides (Fig. 10b).

Decreased CO_2 emissions with Fe^{3+} nitrate additions obtained during the incubation period is due to the form of ions present in the soil solution. The Fe^{3+} and NO_3^- introduced as Fe^{3+} nitrate act as an alternative electron acceptor relative to Fe^{3+} associated with P, DOC and other elements released through mineralization. It is also possible that microorganisms seek Fe^{3+} and nutrients associated with DOC following the depletion of Fe^{3+} nitrate, which is supported by increased CO_2 emissions with Fe^{3+} nitrate addition at 120 DAI (Fig. 5b and c).

The N_2O emissions were detected only under water saturation and waterlogged moisture regimes which could be explained by the release of N under flooded soil which could stimulate N_2O emission [45] and the denitrification occurring under anaerobic conditions where denitrifiers use nitrogen oxides as an alternative electron acceptor [49]. Positive correlations among N_2O and C/N and between N_2O and MBC, MBN, and MBP also demonstrate that dominant sources of N_2O are closely related to soil microbial activity (Fig. 10a). The N_2O emission was not observed under field capacity moisture regime which is due to the prevailing oxidation conditions. Optimum N_2O emissions usually occur under wetter conditions with moisture content >80% water field pore space [16]. Increased N_2O emissions with additions of Fe^{3+} nitrate under water saturation and waterlogged moisture regimes is due to the presence of NO_3^- associated with $Fe(NO_3)_3.9H_2O$, which acts as the substrate for the denitrifiers [49]. The increased N_2O emissions during the first period of incubation and CO_2 after 35 days (Fig. 5f) suggest that the microorganisms have a preference for NO_3^- compare with Fe^{3+} as electron acceptors [18]. As is known, the end products of denitrification (reduction of nitrate) are N_2O and CO_2, whereas the end product of iron reduction is CO_2 [18]. This assumption was confirmed by the inhibition of Fe^{2+} concentration with Fe^{3+} nitrate addition at the first 63 DAI, as the added nitrate was reduced instead of Fe^{3+} during this period. This suggests also that after depleting of O_2, P release to porewater and floodwater might be delay if NO_3^- and other non-related P electron acceptors such as iron addition are present.

4.4. Implications of the study

The past decade has seen an increased number of extreme weather events. Atmospheric rivers and heavy rainfall particularly during the fall in the Fraser valley of BC and other areas of the world have contributed to frequent and extended flooding of agricultural lands. Our results were obtained on soils submitted to extended water saturation and waterlogged moisture regimes. They indicate that frequent and extended flooding of agricultural lands can result to increased concentrations of Pw due to the solubilization of P, the reduction of Fe^{3+} that bind to P, and the release of DOC associated with physically disrupted water-stable aggregates. One consequence is the transport of P and DOC with receding water which would increase the risk of P pollution. We found that MBC and MBN were high in soils under water saturation and waterlogged moisture regimes indicating that C and N were immobilized in microbial biomass due to Fe and Mn oxidation-reduction dynamics which release C that can be used by soil microorganisms and high microbial substrate use efficiency. The reduction reaction in waterlogged soils also enhanced CO_2 and N_2O emissions which could represent hotspots not usually accounted for in estimates of greenhouse emissions from croplands. The addition of Fe^{3+} nitrate inhibited the reduction of Fe^{3+} to Fe^{2+}, decreased Pw, DOC, and CO_2 emission but enhanced N_2O emission at the first period if incubation. These suggest that the microorganisms prefer to use NO_3^- as an electron acceptor compared to Fe^{3+} and the P release into water sources could be delayed by the presence of non-bound P electron acceptors such as Fe^{3+} nitrate addition.

5. Conclusion

We found that pH increased in soils under waterlogged moisture regime as a result of the reduction of Fe^{3+} into Fe^{2+}, but decreased under field capacity. Changes in soil pH with varying moisture regimes also affected the solubility of P. We found increased Pw concentrations under water saturation and waterlogged moisture regimes. In contrast, P_{M3} concentrations were similar in soils under field capacity and water saturation, but lower in soils under waterlogged moisture regimes. The trends of Pw and P_{M3} concentrations under water saturation and waterlogged moisture regimes could be attributed to the interactions between P ions that were previously protected and not exchangeable within water stable aggregates and Fe oxyhydroxides. The dynamics of H^+ cations leading to changes in soil pH is controlled by the status of soil moisture and soil microbial activity as shown by concomitant increased in CO_2 and N_2O emissions, MBC and MBN as well as DOC. The inhibition of the reduction of Fe^{3+} to Fe^{2+} with addition of Fe^{3+} nitrate at the first 63 days could be the result of the added nitrate which is the preferable electron acceptor after O_2 depletion. This assumption was confirmed by the emission of N_2O at the first period of incubation. Addition of Fe^{3+} nitrate decreased Pw at the first 35 DAI, P in floodwater at 120 DAI, and DOC, indicating that the microorganisms used the added Fe^{3+} nitrate as electron acceptor, thus delayed P release into pore water and floodwater.

Author contribution statement

Thidarat Rupngam; Aimé J. Messiga; Antoine Karam: Conceived and designed the experiments; Analyzed and interpreted the data; Wrote the paper.

Thidarat Rupngam; Aimé J. Messiga: Contributed reagents, materials, analysis tools or data; Performed the experiments.

Funding statement

Dr. Aimé J. Messiga was supported by Agriculture and Agri-Food Canada [Project ID: J-002266 - Solutions for carryover of legacy P in the Fraser Valley and Hullcar Valley].

Data availability statement

Data included in article.

Declaration of interest's statement

The authors declare no conflict of interest.

References

[1] A.J. Messiga, C. Lam, Y. Li, Phosphorus saturation index and water-extractable phosphorus in high-legacy phosphorus soils in southern British Columbia, Canada, Can. J. Soil Sci. 101 (2021) 1–13.
[2] R.J. Mitchell, L.M. Braverman, S. Babcock, Transboundary transport in the abbotsford–sumas aquifer, British Columbia and northwestern Washington state, Abstr. Progr. Geol. Soc. Am. 35 (6) (2003) 196–197.
[3] Environment and climate change Canada. Canadian climate normal [Online]. Available from: https://climate.weather.gc.ca/climate_normals/index_e.html. (Accessed 13 March 2022).
[4] K. Zhu, Y. Ran, M. Ma, W. Li, Y. Mir, J. Ran, S. Wu, P. Huang, Ameliorating soil structure for the reservoir riparian: the influences of land use and dam-triggered flooding on soil aggregates, Soil Till. Res. 216 (2022), 105263.
[5] R. Karmakar, I. Das, D. Dutta, A. Rakshit, Potential effects of climate change on soil properties: a review, Sci. Int. 4 (2) (2016) 51–73.
[6] K. Dorau, S. Wessel-Bothe, G. Milbert, H.P. Schrey, D. Elhaus, T. Mansfeldt, Climate change and redoximorphosis in a soil with stagnic properties, Catena 190 (2020), 104528.
[7] R. Scalenghe, A.C. Edwards, E. Barberis, F. Ajmone-Marsan, Are agricultural soils under a continental temperate climate susceptible to episodic reducing conditions and increased leaching of phosphorus? J. Environ. Manag. 97 (2012) 141–147.
[8] G.C. Kowalenko, O. Schmidt, E. Kenney, D. Neilsen, D. Poon, Okanagan Agricultural Soil Study. A Survey of the Chemical and Physical Properties of Agricultural Soils of the Okanagan and Similkameen Valleys in Relation to Agronomic and Environmental Concerns, 2007, p. 130.
[9] K. Reid, K.D. Schneider, Phosphorus accumulation in Canadian agricultural soils over 30 yr, Can. J. Soil Sci. 99 (2019) 520–532.
[10] S. Nyamaizi, A.J. Messiga, J.-T. Cornelis, S.M. Smukler, Effects of increasing soil pH to near-neutral using lime on phosphorus saturation index and water extractable phosphorus, Can. J. Soil Sci. 102 (2022) 929–945, 2022.
[11] P.D.K.D. Jayarathne, D. Kumaragamage, S. Indraratne, D. Flaten, D. Goltz, Phosphorus release to floodwater from calcareous surface soils and their corresponding subsurface soils under anaerobic conditions, J. Environ. Qual. 45 (4) (2016) 1375–1384.
[12] R. Scalenghe, C. A, E. Edwards, Barberis, F. Ajmone-Marsan, Release of phosphorus under reducing and simulated open drainage conditions from overfertilised soils, Chemosphere 95 (2014) 289–294.
[13] K.R. Reddy, R.G. Wetzel, R.H. Kadlec, Biogeochemistry of phosphorus in wetlands, Phosphorus: Agric. Environ. 46 (2005) 263–316.
[14] L. Li, Z. Qu, R. Jia, B. Wang, Y. Wang, D. Qu, Excessive input of phosphorus significantly affects microbial Fe(III) reduction in flooded paddy soils by changing the abundances and community structures of Clostridium and Geobacteraceae, Sci. Total Environ. 607–608 (2017) 982–991.
[15] T. Zhang, S.M. Gannon, K.P. Nevin, A.E. Franks, D.R. Lovley, Stimulating the anaerobic degradation of aromatic hydrocarbons in contaminated sediments by providing an electrode as the electron acceptor, Environ. Microbiol. 12 (2010) 1011–1020.
[16] S. Zechmeister-Boltenstern, G. Schaufler, B. Kitzler, NO, NO_2, N_2O, CO_2 and CH_4 fluxes from soils under different land use: temperature sensitivity and effects of soil moisture, Geophys. Res. Abstr. 8 (2007) 7968.
[17] A.J. Messiga, N. Ziadi, D.A. Angers, C. Morel, L.-E. Parent, Tillage practices of a clay loam soil affect soil aggregation and associated C and P concentrations, Geoderma 164 (2011) 225–231.
[18] P. Inglett, K.R. Reddy, R. Corstanje, soils Anaerobic, in: D. Hillel, J.D. Sachs (Eds.), Encyclopedia of Soils in the Environment, Elsevier Ltd., Columbia University, New York, NY, USA, 2005, pp. 72–78, https://doi.org/10.1016/B0-12-348530-4/00178-8.
[19] Soil Survey Staff, Soil Survey Manual. Soil Conservation Service, USDA, Washington, DC, 2014.
[20] Soil Classification Working Group, The Canadian System of Soil Classification, third ed., Agriculture and Agri-Food Canada Publication 1646, 1998, p. 187pp.
[21] Environment and climate change Canada. Canadian climate normals Agassiz CDA [Online]. Available from: https://climate.weather.gc.ca/climate_normals/results_1981_2010_e.html?stnID=707&autofwd=1. (Accessed 5 October 2021).
[22] A.J. Messiga, X. Hao, N. Ziadi, M. Dorais, Reducing peat in growing media: impact on nitrogen content, microbial activity, and CO2 and N2O emissions, Can. J. Soil Sci. 102 (1) (2021) 77–87.
[23] P. Rochette, N. Bertrand, M. Carter, E.G. Gregorich, Soil-surface Gas Emissions. Soil Sampling and Methods of Analysis, CRC Press, Boca Raton, FL, 2008, pp. 851–861.
[24] W.H. Hendershot, H. Lalande, M. Duquette, Soil reaction and exchangeable acidity, Soil Samp. Meth. Analy. 2 (1993).
[25] C.H. Liu, W. Chu, H. Li, S.A. Boyd, B.J. Teppen, J. Mao, J. Lehmann, W. Zhang, Quantification and characterization of dissolved organic carbon from biochars, Geoderma 335 (2019) 161–169.
[26] M.L. Self-Davis, P.A. Moore Jr., B.C. Joern, Determination of water-and/or dilute salt-extractable phosphorus. Methods of phosphorus analysis for soils, sediments, residuals, and waters, South. Cooper. Bull. 396 (2000) 24–26.
[27] N. Ziadi, T.S. Tran, Mehlich 3-extractable Elements. Soil Sampling and Methods of Analysis, 2008, pp. 81–88.
[28] O.F. Schoumans, Determination of the degree of phosphate saturation in non-calcareous soils, in: second ed.Methods of Phosphorus Analysis for Soils, Sediments, Residuals, and Waters, 2000, pp. 29–32.
[29] C.G. Kowalenko, D. Babuin, Use of lithium metaborate to determine total phosphorus and other element concentrations in soil, plant, and related materials, Commun. Soil Sci. Plant Anal. 45 (2014) 15–28.
[30] B.J. Cade-Menun, I.P. O'Halloran, Total and organic phosphorus, in: second ed.Soil Sampling and Methods of Analysis, CRC Press, Taylor & Francis, Boca Raton, FL, 2007, pp. 265–292.
[31] J. Murphy, J.P. Riley, A modified single solution method for the determination of phosphate in natural waters, Anal. Chem. Acta 27 (1962) 31–36.
[32] S.E.A.T.M. Van der Zee, V.D.L. Fokkink, W.H.A. Van Riemsdijk, New technique for assessment of reversibly adsorbed phosphate, Soil Sci. Soc. Am. J. 51 (3) (1987) 599–604.
[33] L. Khiari, L.E. Parent, A. Pellerin, A.R.A. Alimi, C. Tremblay, R.R. Simard, J. Fortin, An agri-environmental phosphorus saturation index for acid coarse-textured soils, J. Environ. Qual. 29 (5) (2000) 1561–1567.
[34] R. Benjannet, L. Khiari, J. Nyiraneza, B. Thompson, J. He, X. Geng, K. Stiles, Y. Jiang, S. Fillmore, Identifying environmental phosphorus risk classes at the scale of Prince Edward Island, Canada, Can. J. Soil Sci. 98 (2) (2018) 317–329.
[35] W. Yu, N.C. Lawrence, T. Sooksa-Nguan, S.D. Smith, C. Tenesaca, A.C. Howe, S.J. Hall, Microbial linkages to soil biogeochemical processes in a poorly drained agricultural ecosystem, Soil Biol. Biochem. 156 (2021), 108228.
[36] W. Huang, S.J. Hall, Optimized high-throughput methods for quantifying iron biogeochemical dynamics in soil, Geoderma 306 (2017) 67–72.
[37] J.F. Vizier, Étude de l'état d'oxydo-réduction du sol et de ses conséquences sur la dynamique du fer dans les sols hydromorphes, Bulletin de Liaison du Thème C-ORSTOM (1) (1971) 19–64.
[38] R.P. Voroney, P.C. Brookes, R.P. Beyaert, Soil microbial biomass C, N, P, and S, Soil Samp. Meth. Analy. 2 (2008) 637–652.

[39] P.A. Moore, K.R. Reddy, Role of Eh and pH on phosphorus geochemistry in sediments of Lake Okeechobee, Florida, J. Environ. Qual. 23 (1994) 955–964.
[40] H.L. Lu, K.W. Li, J.N. Nkoh, X. He, R.K. Xu, W. Qian, R.Y. Shi, Z.N. Hong, Effects of pH variations caused by redox reactions and pH buffering capacity on Cd (II) speciation in paddy soils during submerging/draining alternation, Ecotoxicol. Environ. Saf. 234 (2022), 113409.
[41] Y. Pan, G.F. Koopmans, L.T. Bonten, J. Song, Y. Luo, E.J. Temminghoff, R.N. Comans, Influence of pH on the redox chemistry of metal (hydr) oxides and organic matter in paddy soils, J. Soils Sediments 14 (10) (2014) 1713–1726.
[42] P. Boivin, F. Favre, C. Hammecke, J.L. Maeght, J. Delariviere, J.C. Poussin, M.C.S. Wopereis, Processes driving soil solution chemistry in a flooded rice cropped vertisol: analysis of long-time monitoring data, Geoderma 110 (2002) 87–107.
[43] P. Hinsinger, Bioavailability of soil inorganic P in the rhizosphere as affected by root-induced chemical changes: a review, Plant Soil 237 (2001) 173–195.
[44] S. Gu, G. Gruau, R. Dupas, P. Petitjean, Q. Li, G. Pinay, Respective roles of Fe-oxyhydroxide dissolution, pH changes and sediment inputs in dissolved phosphorus release from wetland soils under anoxic conditions, Geoderma 338 (2019) 365–374.
[45] M. Shaaban, M.S. Khalid, R. Hu, M. Zhou, Effects of water regimes on soil N2O, CH4 and CO2 emissions following addition of dicyandiamide and N fertilizer, Environ. Res. 212 (2022), 113544.
[46] L. Wei, T. Ge, Z. Zhu, R. Ye, J. Penuelas, Y. Li, T.M. Lynn, D.L. Jones, J. Wu, Y. Kuzyakov, Paddy soils have a much higher microbial biomass content than upland soils: a review of the origin, mechanisms, and drivers, Agric. Ecosyst. Environ. 326 (2022), 107798.
[47] M. Mooshammer, W. Wanek, J. Schnecker, B. Wild, S. Leitner, F. Hofhansl, A. Blöchl, I. Hämmerle, A.H. Frank, L. Fuchslueger, K.M. Keiblinger, S. Zechmeister-Boltenstern, A. Richter, Stoichiometric controls of nitrogen and phosphorus cycling in decomposing beech leaf litter, Ecology 93 (4) (2012) 770–782.
[48] M. Rantakari, P. Kortelainen, Interannual variation and climatic regulation of the CO2 emission from large boreal lakes, Global Change Biol. 11 (2005) 1368–1380.
[49] K. Butterbach-Bahl, E.M. Baggs, M. Dannenmann, R. Kiese, S. Zechmeister-Boltenstern, Nitrous oxide emissions from soils: how well do we understand the processes and their controls? Philos. Trans. R. Soc. B: Biol. Sci. 368 (1621) (2013), 20130122.